Acta Scientiarum

http://www.uem.br/acta
ISSN printed: 1806-2563
ISSN on-line: 1807-8664
Doi: 10.4025/actascitechnol.v37i2.20317

Principle and geomorphological applicability of summit level and base level technique using Aster Gdem satellite-derived data and the original software Baz

Akihisa Motoki[1], Kenji Freire Motoki[2], Susanna Eleonora Sichel[2], Samuel da Silva[2] and José Ribeiro Aires[3*]

*[1]Universidade Estadual do Rio de Janeiro, Rua São Francisco Xavier, 524, 20550-990, Maracanã, Rio de Janeiro, Brazil. [2]Universidade Federal Fluminense, Niterói, Rio de Janeiro, Brazil. [3]Petrobras, Rio de Janeiro, Rio de Janeiro, Brazil. [†]In memoriam. *Author for correspondence. E-mail: aires@petrobras.com.br*

ABSTRACT. This article presents principle and geomorphological applicability of summit level technique using Aster Gdem satellite-derived topographic data. Summit level corresponds to the virtual topographic surface constituted by local highest points, such as peaks and plateau tops, and reconstitutes palaeo-geomorphology before the drainage erosion. Summit level map is efficient for reconstitution of palaeo-surfaces and detection of active tectonic movement. Base level is the virtual surface composed of local lowest points, as valley bottoms. The difference between summit level and base level is called relief amount. These virtual maps are constructed by the original software Baz. The macro concavity index, MCI, is calculated from summit level and relief amount maps. The volume-normalised three-dimensional concavity index, TCI, is calculated from hypsometric diagram. The massifs with high erosive resistance tend to have convex general form and low MCI and TCI. Those with low resistance have concave form and high MCI and TCI. The diagram of TCI vs. MCI permits to distinguish erosive characteristics of massifs according to their constituent rocks. The base level map for ocean bottom detects the basement tectonic uplift which occurred before the formation of the volcanic seamounts.

Keywords: summit level, base level, morphological analyses, palaeo-surface, erosive resistance, active fault.

Princípio e aplicabilidade das técnicas de seppômen e sekkokumen para análises geomorfológicas com base nos dados de satélites do Aster Gdem e o software original Baz

RESUMO. Este artigo apresenta o princípio e a aplicabilidade geomorfológica da técnica de seppômen e sekkokumen utilizando-se os dados topográficos de satélite do Aster Gdem. O seppômen corresponde à superfície topográfica virtual constituída por pontos culminantes locais, tais como picos e topos de platôs, e reconstitui a paleogeomorfologia antes da erosão por drenagens. O mapa de seppômen é eficiente para reconstituição de paleossuperfícies e detecção de movimentos tectônicos ativos. O sekkokumen é a superfície virtual composta de pontos locais mais baixos, como fundo de vales. A diferença entre seppômen e sekkokumen é denominada kifukuryô. Esses mapas virtuais são elaborados pelo software original Baz. O índice de macro concavidade de maciço, MCI, é calculado a partir dos mapas de seppômen e kifukuryô. O parâmetro de convexidade tridimensional normalizado por volume, TCI, é calculado por diagrama hipsométrico. Os maciços com alta resistência erosiva tendem a ter forma geral convexa e altos MCI e TCI. Aqueles com baixa resistência erosiva possuem forma côncava e baixos MCI e TCI. O diagrama de TCI v.s. MCI permite distinguir as características erosivas do maciço de acordo com as rochas constituintes. A técnica de sekkokumen aplicada ao fundo do oceano detecta o soerguimento tectônico do embasamento que ocorreu antes da formação dos montes submarinos vulcânicos.

Palavras-chave: nível de pico, nível de base, análise morfológica, paleossuperfície, resistência erosiva, falha ativa.

Introduction

Summit level and base level technique are efficient instruments for geomorphologic analyses, especially those related to neotectonic movement (MARTIN, 1966; HUZITA; KASAMA, 1977; DEFFONTAINES et al., 1994; RIIS, 1996; FERHAT et al., 1998; KÜHNI; PFIFFENER, 2001; SATO; RAIM, 2004; RÖMER, 2008; MOTOKI et al., 2009a), eroded volcanic edifices (VILARDO et al., 1996; MALENGREAU et al., 1999; RUST et al., 2005; OKUMA et al., 2009), and erosive resistance (MOTOKI et al., 2008a; AIRES et al., 2012).

Summit level map (seppômen) represents the virtual topographic surface constituted by local

highest point, such as peaks and plateau tops. It shows the palaeo geomorphology before vertical erosion of valleys and drainages. Base level map (sekkokumen) constructed by the surface composed of the local lowest points, as valley and basin bottoms. It predicts the future geomorphology which will be formed by lateral erosion of the drainages. Either summit level or base level maps are elaborated from topographic map.

Summit level technique has been developed since decade of 1950, mainly by Japanese researchers of natural geography. At the present, it is used by Japanese municipal and provincial governments as a fundamental instrument for natural disaster predictions and mitigations, especially for landslides and debris flows caused by heavy rainfalls.

In Brazil, summit level technique was introduced for the morphologic analyses of Poços de Caldas alkaline intrusive complex, State of Minas Gerais, in order to examine if the present morphology is originated from a volcanic caldera or differential erosion of felsic alkaline intrusive rocks. The Mendanha alkaline intrusive body, State of Rio de Janeiro, was studied using summit level technique to verify if it is a volcanic edifice with cone and crater or an intrusive massif originated from differential erosion of felsic alkaline rocks (MOTOKI et al., 2008a). Recently, the felsic alkaline intrusive complexes of Morro do São João and Tanguá, State of Rio de Janeiro (MOTOKI et al., 2014a; 2015a and b), were studied for the purpose of morphologic comparison with gneissic and granitic massifs. Couto et al. (2012) applied summit level technique for Quaternary tectonic movement in the Paraná Plateau border areas.

This paper shows the principle and methodology of summit level and base level technique and their applicability for morphological analyses based on the available published articles, submitted papers, and new data of the studies in development. In addition, the authors discussed possible future technical developments, proposing new parameters.

Principle of the techniques

In the initial stage of the erosion cycle of Davis (1899), narrow and deep drainages are formed grooving original elevated peneplain. This phase is called young stage and the original surface is preserved in a large and continuous area. Therefore, the original elevated peneplain can be reconstituted by drainage fill. Summit level map was created for this purpose (Figure 1).

In an area with more relevant erosion, the original surface is preserved only at small and separated areas. Even in this case, summit level map can reconstitute the original plain, but less precisely. The older morphologic information is less preserved.

In stage of more advanced erosion, called the mature stage, the original surface is no more preserved and reconstitution of the original surface is not possible. In an area of much more advanced erosion, called old stage, vertical erosion is not important and lateral erosion becomes expressive. In the peneplain stage, summit revel map show the virtual surface formed by the top of monadonocks, indicating erosive resistance of the constituent rocks.

Summit level map is useful to detect vertical displacement of active fault, especially in areas of the young stage. It is efficient also for the reconstruction of original morphology of eroded volcanic edifices and impact craters.

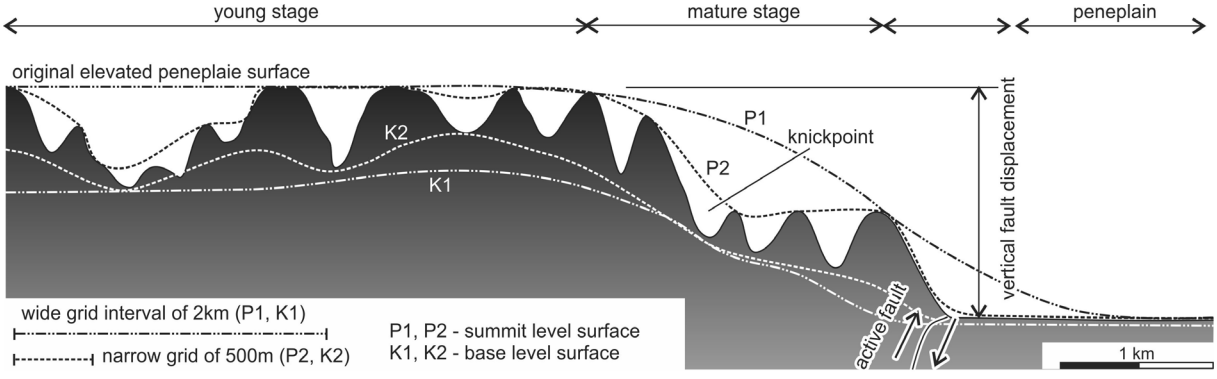

Figure 1. Principle of summit level and base level technique and effects of grid interval, modified from Motoki et al. (2008a).

On the other hand, base level map shows erosive tendency indicating three-dimensional longitudinal section of valleys, being useful to study knickpoints. In the oceanic regions, it expresses basement height of seamounts, with similar effect of the Wiener low-pass filter (SMITH; SANDWELL, 1994).

Construction method of the virtual maps

There are two main methods for the construction of summit level maps, which are grid method (*Hogan-hô*) and valley-fill method (*maikoku-hô*). The grid method is convenient for the data of digital topographic model, called DEM, and digital computing. The summit level map by the grid method is confected by the following steps (Figure 2): 1) Divide the original topographic map into small square areas by a grid of defined interval; 2) Mark the highest point of each square; 3) Construct a new topographical map using the marked points. Base level map is elaborated by similar processes but using the lowest point of the squares. The difference between them is called relief amount and it is related to local declivity.

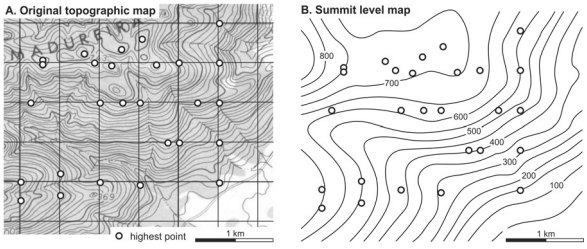

Figure 2. Confection procedures of summit level map by means of the grid method (*Hôgan-hô*) after Motoki et al. (2008a). The grid interval is 500 m.

The authors adopt Aster Gdem moderated by SRTM for the original topographic data, which are released from the United States Geological Survey. The virtual maps are constructed by the original software Baz version 1.0 (MOTOKI et al., 2012a) and Wilbur version 1.0 (MOTOKI et al., 2005; 2006; 2007a). They run on the DOS platform by line-command, so the operations are not familiar for Windows™ users.

Grid interval is an important factor for the virtual maps. The summit level maps based on a narrow grid show detailed palaeo-geomorphology of a near past. On the other hand, those based on a wide grid interval demonstrate palaeo-geomorphology of a remote past in ambiguous way (Figure 1). Similar tendencies occur in base level maps. The software BAZ constructs simultaneously the virtual maps of summit level, base level, and relief amount of various grid intervals, revealing geomorphologic evolution history.

The valley-fill method is convenient for analogue data treatment by manual works from the paper-printed topographic map (MOTOKI et al., 2008a; 2009a). The summit level maps are elaborated filling the drainages narrower than the threshold width (Figure 3). The base level map is elaborated eliminating the ridges narrower than the threshold. The threshold length of valley-fill method has similar significance of the grid interval of grid method.

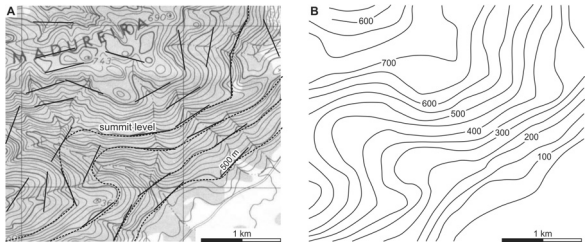

Figure 3. Confection procedures of summit level map by the valley-fill method (*maikoku-hô*). The threshold width for this map is 500 m.

Palaeo-surface reconstitution

Reconstitution of palaeo-surfaces is the primary and most important function of summit level technique and detects Cenozoic tectonic movement form the topographic characteristics. The Figure 4 presents summit level map for the central region of State of Rio de Janeiro, Brazil, based on grid interval of 4 km (AIRES et al., 2012). The Figure 5 shows the morphotectonic interpretation with special attention of Cenozoic tectonism.

Almeida and Carneiro (1998) and Zalán and Oliveira (2005) interpreted that Serra do Mar Scarp was formed by vertical displacement of the normal fault related to the continental rift of the Atlantic Ocean opening during the Cretaceous to the early Cenozoic. The fault movement and the consequent fault scarp formation were originated from the continental crust thinning. The tectonism occurred mainly in a period of 52 to 40 Ma (FERRARI, 2001; RICCOMINI et al., 2004).

The fault displacement divided the original surface of the Cretaceous into two levels, Fluminense Lowland (Baixada Fluminense) and Teresópolis Highland (Planalto de Teresópolis). The basement level of Fluminense Lowland is represented by the summit level surface of 100 m of altitude. The Teresópolis Highland is represented by the summit level surface of 1300 m of altitude. This plateau surface shows gentle tilting of 0.9º to the north-west, called the Paraíba do Sul tilted block. The Serra do Mar Scarp is originated from the vertical displacement of 1200 m. Along the scarp, some mega-landslide blocks are observed in the summit level map of the grid interval of 2 and 1 km.

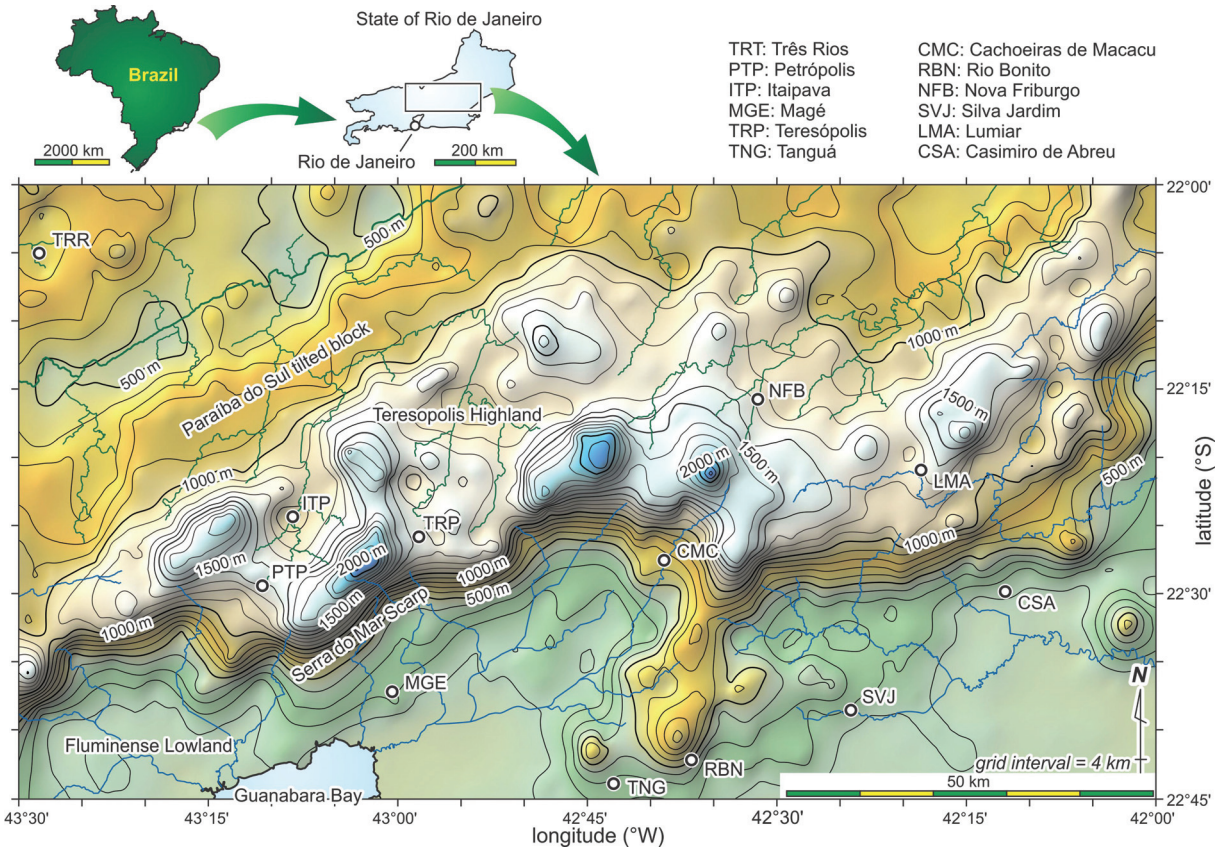

Figure 4. Summit level map for the central region of State of Rio de Janeiro State, Brazil, based on grid interval of 4 km (AIRES et al., 2012).

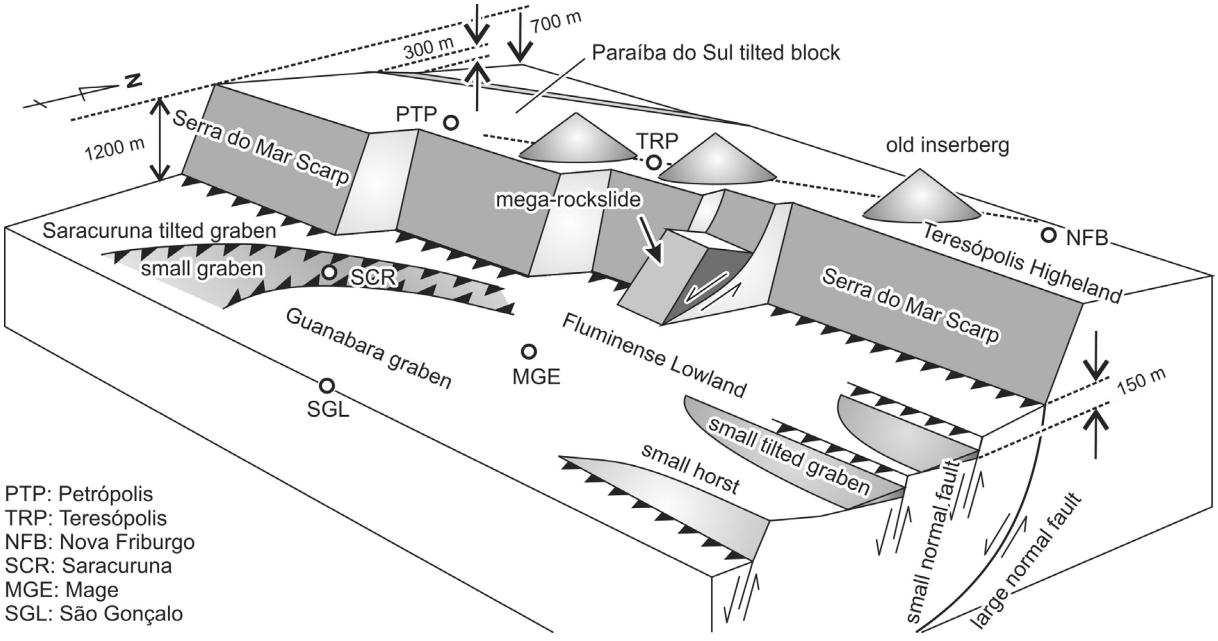

Figure 5. Schematic illustration for the Cenozoic tectonism in the central region of State of Rio de Janeiro State, interpreted from the summit level maps (AIRES et al., 2012).

After the events of continental thinning and the consequent opening of Atlantic Ocean in the late Mesozoic, this area has been uplifted by isostatic compensation. The fission-track dating for apatite permits to estimate the total uplift vertical movement as ca. 3 km (MOTOKI et al., 2012b; 2007b).

The summit level map is quite efficient for the areas of Quaternary tectonism. The neotectonic study of the Mount Rokko, Kobe, Japan (HUZITA; KASAMA, 1977), was a pioneer work using summit level technique. The Figure 6 shows the summit level map of grid interval of 490 m using the updated topographic data of the Aster Gdem.

The elevated peneplain of Mount Rokko has maximum altitude of 932 m and its southeast border is limited by a series of NE-SW trend composed of Suma, Suwayama, and Gosukebashi fault (LIN et al., 1998; MARUYAMA; LIN, 2000). They are named collectively Kobe Fault System and have right-lateral component with total displacement of 1.7 km (MOTOKI, 1979; 1994). The horizontal displacement component is 4 times larger than the vertical one. The vertical component is small in the western span, about 200 m along Suma Fault, and becomes larger to the east, about 550 m, along Gosukebashi Fault. This map detects 4 levels of the elevated peneplain, called Rokko, Okuike, Taishaku, and Suzurandai surface, with respective altitudes of 900, 550, 550, and 400 m. All of them show general tilting to the west, with approximate declivity of 2º.

The summit level technique is very important for the areas of Holocene tectonism. At the Saint Peter and Saint Paul Islets of the Equatorial Atlantic Ocean, the most intense active uplift of Brazil is observed (MOTOKI et al., 2009a; MOTOKI et al., 2014a). In this area, the ENE-WSW trend transform fault is exceptionally not parallel to the E-W ward relative motion between South American Plate and African Plate, with maximum angular discordance of 25º (SICHEL et al., 2011). The directional discrepancy generates near N-S compression stress, and it has squeezed the mantle peridotite out of the ductile deformation depth (SICHEL et al., 2008a) up to the sea level.

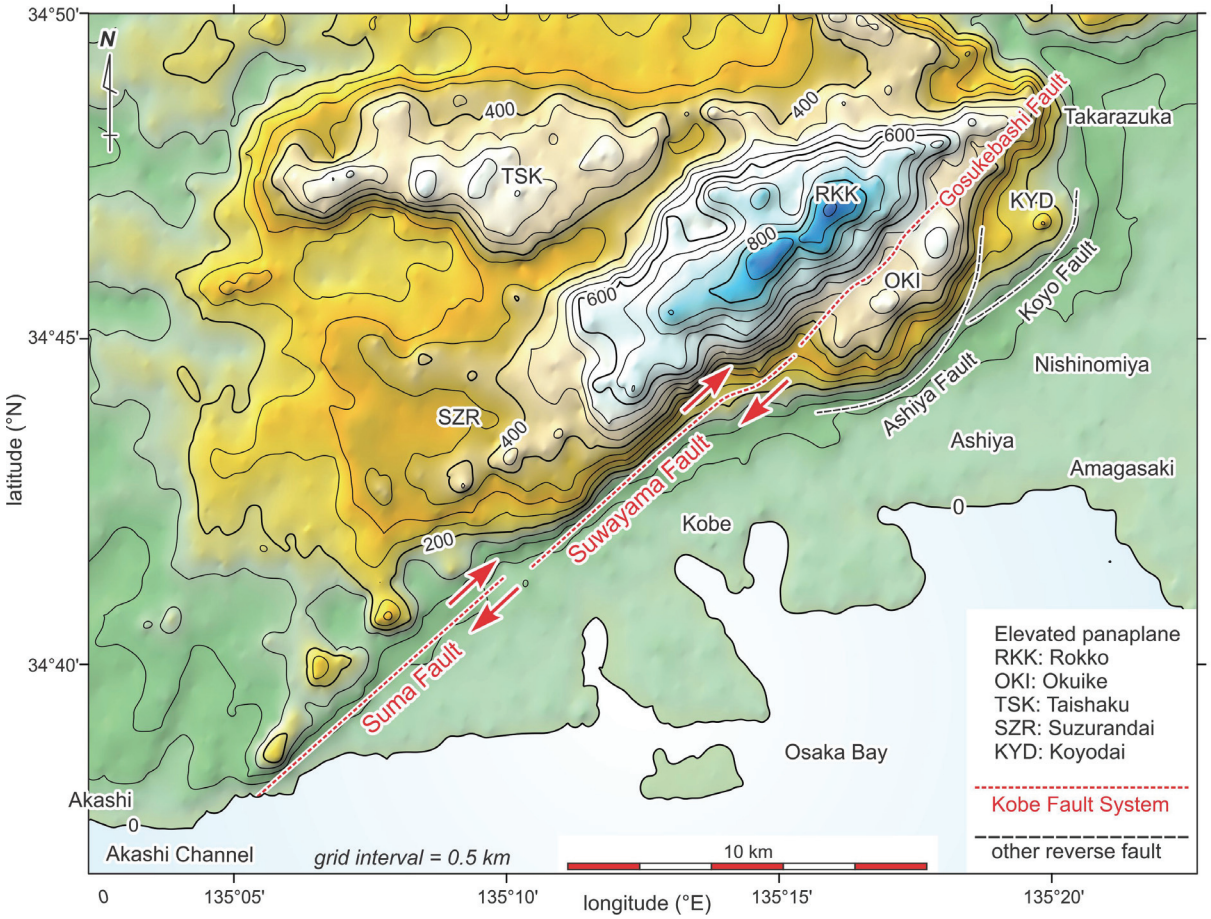

Figure 6. Summit level map of grid interval of 0.5 km for Mount Rokko, Kobe, Japan, based on the updated data of the Aster Gdem moderated by the SRTM. Because of the confection process of the map, the positions of coast line are not precise.

The Figure 7 presents the summit level map for the Saint Peter and Saint Paul Islets, which was confected by valley-fill method with the threshold width of 10 m. The map shows two levels of wave-cut bench, called the Upper bench, from 7 to 10 m above sea level, and the Lower bench, from 4 to 6 m. The Upper bench was generated during the Flandrian Transgression in ca. 6000 years ago, and indicates average uplift rate of 1.5 mm year^{-1}. The ^{14}C datings for the biogenic carbonates support this rate (CAMPOS et al., 2010). O the other hand, the Lower bench is under the on-going wave-cut erosion.

Reconstitution of volcanic calderas

On the Earth's surface, there are circular morphologic depressions larger than 1 km of diameter. Most of them are originated from volcanic caldera or impact carter. There also are the geologic structure originated from caldera or meteorite crater. Among these morphologic depressions, the former two have similar characteristics, but the latter is notably different. According to the passage of time, the original morphology deteriorates by erosion and become ambiguous. But the original surface can be reconstituted, at least partially, by summit level technique.

The Figure 8 presents summit level maps for the Aso Caldera, Kyushu, Japan, Valles Caldera, New Mexico, USA, Kilauea Caldera, Hawaii, USA, and Poços de Caldas felsic alkaline intrusive body, Minas Gerais State, Brazil, which represent respectively Krakatoa type caldera, Valles type caldera, Kilauea type caldera, and felsic alkaline intrusive rock body. The Figure 9 shows their cross section.

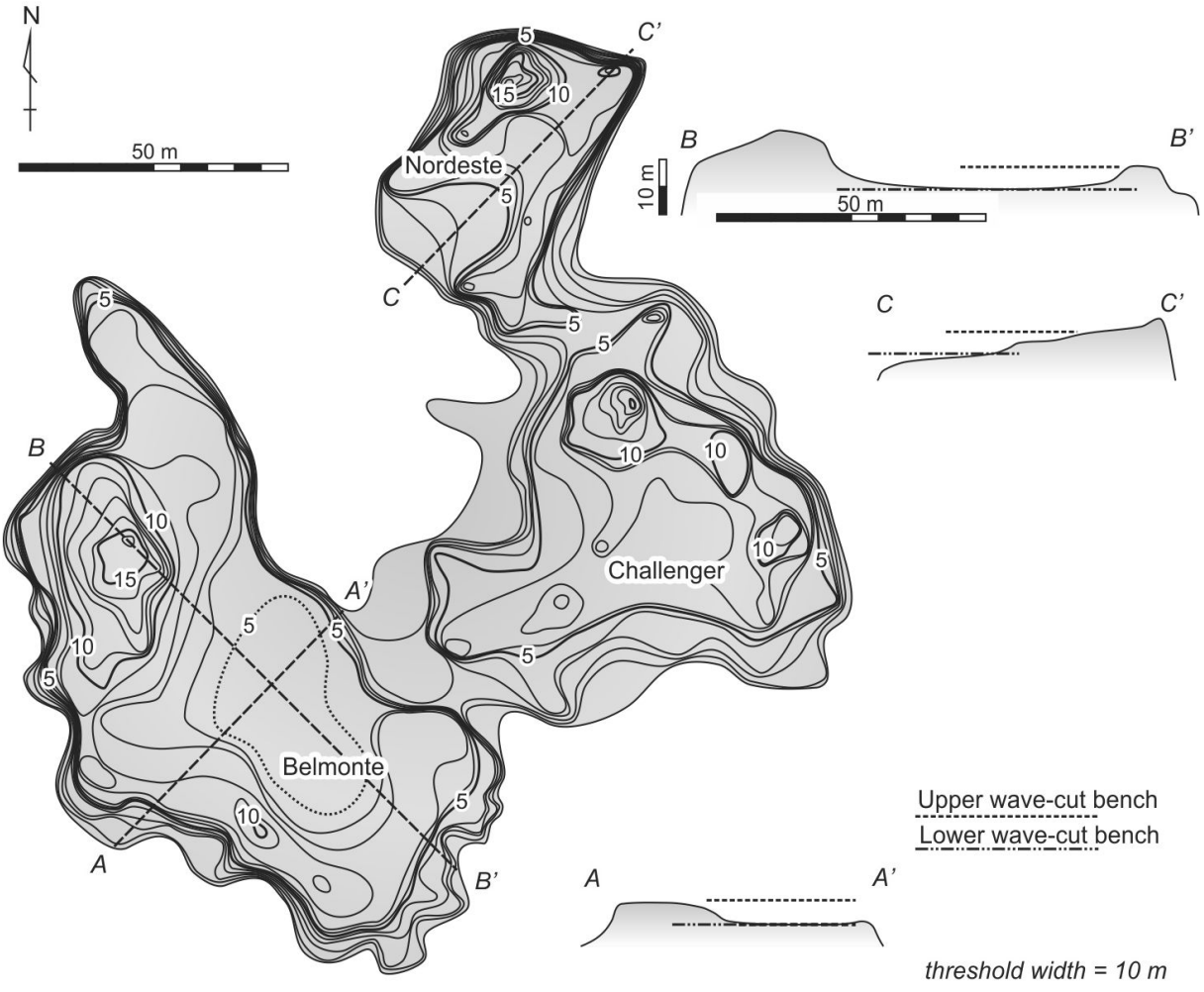

Figure 7. Summit level map for the Saint Peter and Saint Paul Islets, Equatorial Atlantic Ocean, constructed by valley-fill method with threshold width of 10 m (MOTOKI et al., 2009a).

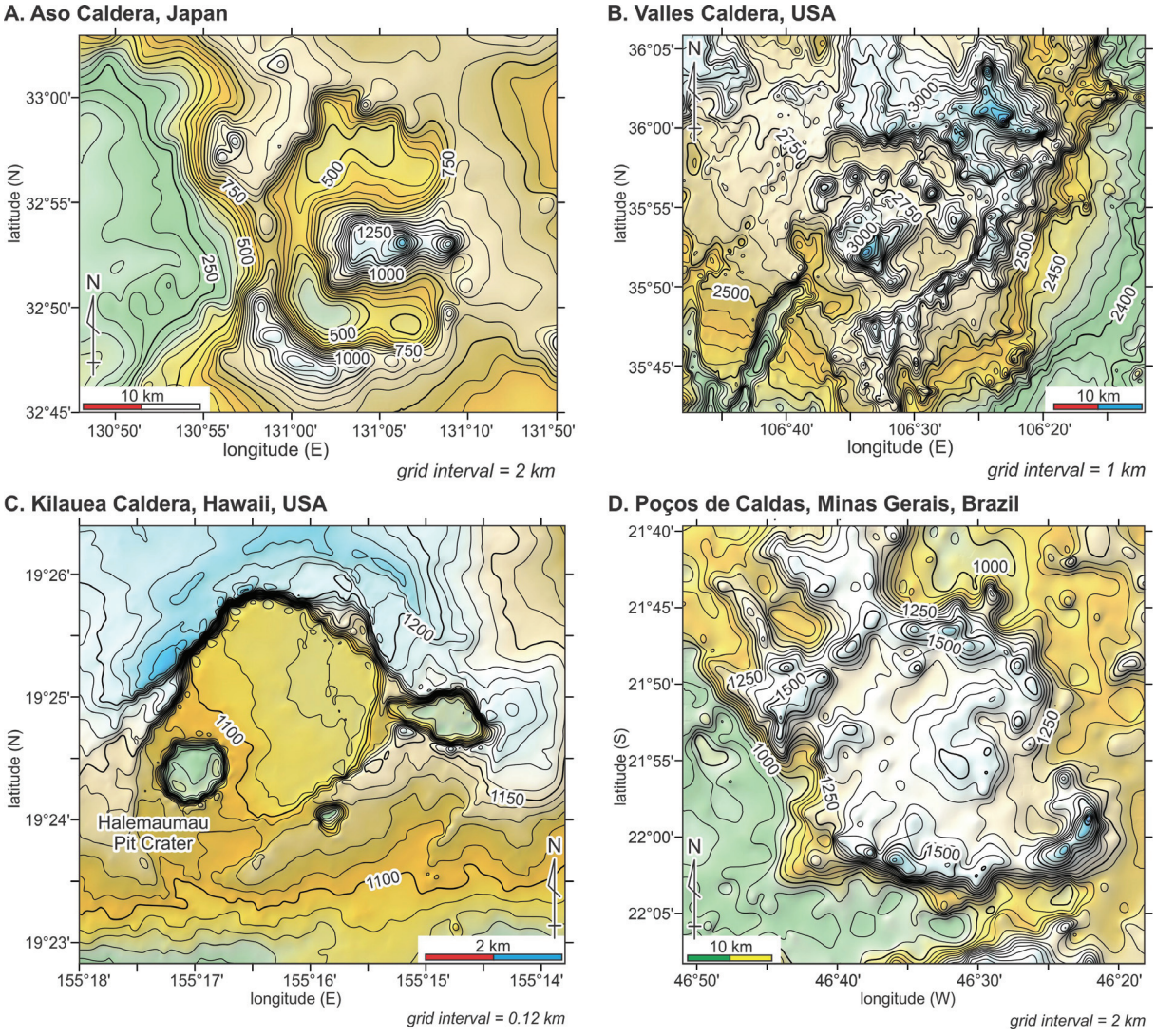

Figure 8. Summit level maps for volcanic calderas and felsic alkaline intrusive body: A) Aso Caldera, Kyushu, Japan; B) Valles Caldera, New Mexico, USA; C) Kilauea Caldera, Hawaii, USA; D) Poços de Caldas felsic alkaline intrusive body, Minas Gerais State, Brazil.

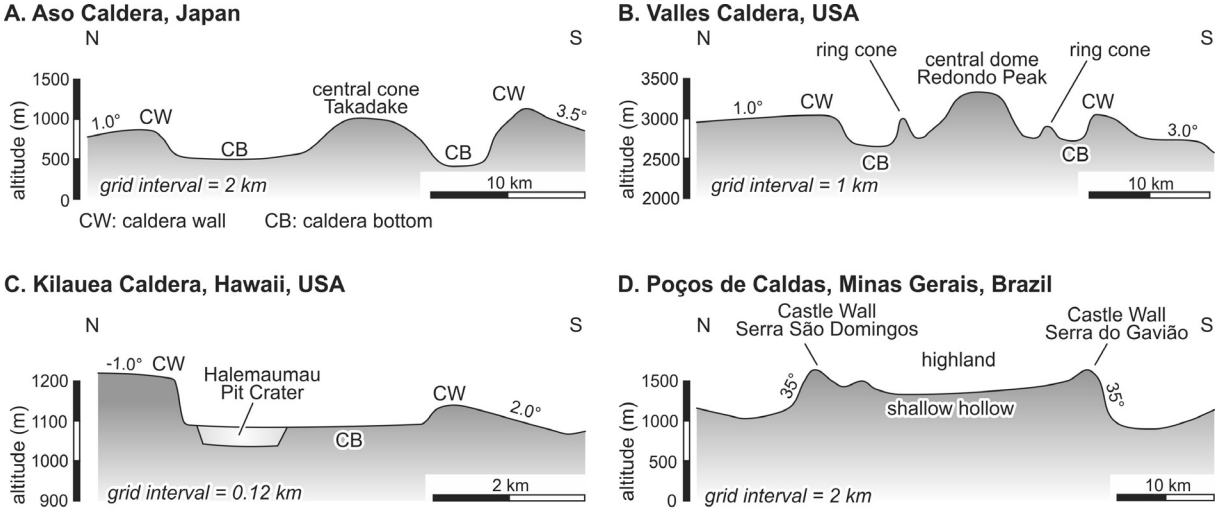

Figure 9. Vertical cross section of the summit level surface for volcanic calderas and felsic alkaline intrusive body: A) Aso Caldera; B) Valles Caldera; C) Kilauea Caldera; D) Poços de Caldas felsic alkaline intrusive body.

The Aso Caldera takes place in the central region of the Kyushu Island, Japan. The circular depression has 25 x 18 km with depth of about 400 m. The caldera bottom is flat due to old caldera lake deposits. This lake was broken by the drainage of western border of the caldera, called Shirakawa River. There are E-W trend central cones with maximum relative height of 1200 m. The last caldera formation event of explosive eruption occurred at 90 Ka (WATANABE, 1978). The summit level map of grid interval of 2 km shows a closed depression area. The caldera wall is steep, of about 30º of declivity. The areas out of the caldera wall are covered by the Aso IV pyroclastic flow deposit in a wide area with extension more than 20 km. Its surface is eroded by small drainages. The original surface reconstituted by summit level technique has gentle outward declivity of 1 to 3.5º (Figure 9A). Such a declivity is common in pyroclastic plateau surfaces (SUZUKI-KAMATA; KAMATA, 1990).

The Valles Caldera occurs in State of New Mexico, USA, which has 19 km of diameter and 400 m of depth. The last stage of the caldera formation eruption took place at 1.2 Ma. There are central resurgent lava dome, called Redondo Peak, with relative height of 700 m, and seven post-caldera cones of ring layout (SMITH; BAILEY, 1966; MACDONALD; PALMER, 1990). The volcanic morphology in the caldera is complex and the caldera bottom is divided into 3 basins. The old caldera lake was broken through the drainage of south-western border, called Valle Grande. The caldera wall is steep with 30º of declivity. The areas out of the caldera wall are underlain by the Bandelier Tuff pyroclastic flow deposit in a wide area with extension more than 30 km. Its surface shows more advanced erosion than the case of Aso Caldera because of the older age. The pyroclastic deposit surface reconstituted by summit level technique expresses outward declivity of 1 to 3º (Figure 9B).

The Krakatoa type and Valles type calderas are formed by explosive eruption of felsic magma and have negative Bouguer gravimetric anomaly (YOKOYAMA; TAJIMA, 1959; 1960; YOKOYAMA; SAITO, 1965; YOKOYAMA, 1965; 1969) due to pyroclastic fallout deposits. On the other hand, Kilauea type calderas are formed by basaltic effusive eruption with positive Bouguer anomaly because of the subjacent basaltic intrusive body. The Kilauea Caldera occurs in the south region of Hawaii Island and has extension of 3 x 4 km and depth of 120 m. The Halemaumau Pit Crater, which is filled by the lava of the eruption in 1974, has 500 m of diameter and 60 m of depth. The caldera bottom is flat representing lava lake surface. The lavas in the caldera depression flowed out crossing over the south-western border. The caldera wall is sub-vertical. The areas out of the caldera wall are covered by young lava flows almost without erosion effect. Therefore, the topographic surface and summit level one are almost the same. The lava surface demonstrates outward declivity of -1 to 2º (Figure 9C).

The above-mentioned examples express the following morphologic characteristics of volcanic calderas: 1) Caldera bottom is flat; 2) Only one outlet drainage is present; 3) Caldera wall is steep with declivity of about 30º; 4) The areas out of the caldera wall are covered by extensive pyroclastic deposits or lava flows with extension of more than 20 km; 5) The surface of these eruptive deposits has gentle outward declivity of about 3º.

On the other hand, Poços de Caldas felsic alkaline highland (Planalto de Poços de Caldas), with intrusive age of about 85 Ma (ULBRICH, 1984), is situated at the limit between the State of Minas Gerais and São Paulo, Brazil. The massif has geologic and morphologic characteristics widely different from the above-mentioned volcanic calderas. The main constituent rocks are holocrystalline aegirine phonolite, so-called tinguaite, nepheline syenite, and vent-filling intrusive pyroclastic rocks. The summit level map of 2 km of grid interval shows that its morphologic features are unlikely for a volcanic caldera.

The circular morphologic depression is 30 x 28 km of extension with maximum depth of 300 m. The alkaline massif has 5 outlet drainages. The basin depth of 300 m is too small in comparison with the 30 km of diameter. The basin bottom is not flat but characterised by small hills with relative height of 150 m. This height corresponds to a half of the basin depth. The southern half of the basin is about 100 m higher than northern half. Along the northern and southern border of the intrusive body, there are arc-like ridges, so-called Castle Wall, which mark the border of the basin. The western border is ambiguous and the eastern border has no morphologic characteristics. The inner scarp of the Castle Walls has declivity of 15º and the outer scarp has declivity of 35º, which is steeper than the inner scarp. The areas out of the Castle Wall expose metamorphic rocks of the basement, without the extensive pyroclastic deposits with gentle declivity surface.

On the contrary of the volcanic calderas and meteorite craters, the circular morphologic structure is about 350 m higher than the surrounding areas. That is, the morphology of Poços de Caldas

highland is not a crater-like circular depression but a wood stock-shaped circular protrusion with shallow saucer-shaped hollow on the top surface (Figure 9D). Theses morphologic characteristics are similar to those of felsic alkaline intrusive massifs of Poços de Caldas-Cabo Frio magmatic alignment, which are originated from differential erosion, and not to those of the volcanic calderas.

Macro concavity index

In areas of mature and old stages, summit level maps provide information about erosive resistance of the base rock. This map also shows the geologic anomalies reflected to the morphology. The combination of summit level and base level techniques provides quantitative index of erosive resistance of the target massif.

The macro concavity index, called MCI, indicates quantitatively general form of the massif if it is convex or concave. It is defined on the diagram of summit level vs. relief amount, called MCI diagram. The projected points are represented by second order polynomial regression. The MCI corresponds to 1000 times of the 'a' constant of the of the quadric equation $y = \mathbf{a}x^2 + bx + c$ (MOTOKI et al., 2012a; 2014b; 2015a; b). The massifs of young stage of erosion have negative MCI and those of advanced stage have positive MCI.

This parameter is efficient to characterise erosive morphology of felsic alkaline intrusive massifs. State of Rio de Janeiro has more than 10 intrusive bodies of nepheline syenite and alkaline syenite (SICHEL et al., 2012), such as Itatiaia (BROTZU et al., 1997; PIRES et al., 2014), Morro Redondo (BROTZU et al., 1989), Serra de Tomases, Tinguá (DERBY, 1897), Mendanha (MOTOKI et al., 2007c), Itaúna (MOTOKI et al., 2008b), Tanguá, Rio Bonito, Soarinho (MOTOKI et al., 2010), Morro dos Gatos (MOTOKI et al., 2012c; GERALDES et al., 2013), Morro de São João (BROTZU et al., 2007), and Cabo Frio Island (MOTOKI; SICHEL, 2008; MOTOKI et al., 2008c). Some of them accompany subvolcanic pyroclastic conduits and fissures (MOTOKI et al., 2007d; SICHEL et al., 2008b). All of them are intrusive pyroclastic bodies without extrusive bodies are observed (MOTOKI; SICHEL, 2006; MOTOKI et al., 2008d).

Their basement is constituted by Pan-African orthogneiss (HEILBRON et al., 2000; HEILBRON; MACHADO, 2003), paragneiss (VALLADARES et al., 2008), Post-tectonic granite (VALERIANO et al., 2011), silicified tectonic breccia (MOTOKI et al., 2011; 2012d), and early Cretaceous mafic dykes (BENNIO et al., 2003; MOTOKI et al., 2009b). Most of the basement rocks contain significant amount of quartz and this mineral is resistant to weathering. On the other hand, the felsic alkaline rocks are constituted mainly by alkaline feldspar and nepheline, which are vulnerable to chemical weathering, transforming easily into clay minerals.

Nevertheless, the above-mentioned alkaline intrusive bodies stand up on the basement peneplain forming morphologic elevations with relative height of 300 to 900 m, so-called alkaline massifs. This apparently controversial phenomenon is due to clay-rich impermeable regolith originated from the alkaline rocks which protects the rock body from surface water percolation, the phenomenon called weathering passivity (PETRAKIS et al., 2010; SILVA, 2010).

The Figure 10 shows the MCI diagram, which demonstrates the strong morphologic contrast between alkaline massifs and young volcanoes. The alkaline massifs have remarkable negative MSI and the convex three-dimensional landforms because of strong erosive resistance of massive plutonic rocks. On the other hand, the active and young volcanoes have positive MCI, demonstrating concave three-dimensional landforms because of the original form of volcanic edifice.

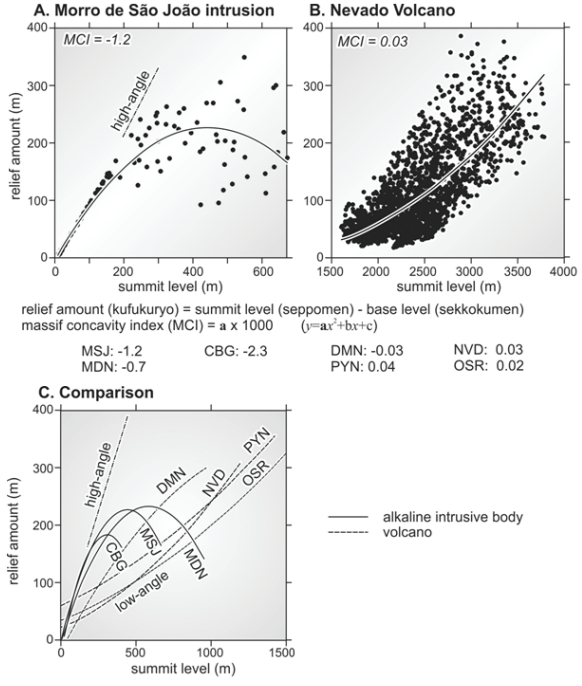

Figure 10. MCI diagram for the alkaline massifs and young volcanic edifices based on grid interval of 480 m, modified from Motoki et al. (2012a). MSJ - Morro de São João alkaline massif; MND - Mendanha alkaline massif (Rio de Janeiro State, Brazil); CBG - Cabugi Peak (Rio Grande do Norte State, Brazil); DMN - Cerro de Diamante, NVD - Nevado; PYN - Payún Liso (Mendoza, Argentina), OSR - Osorno (Chile).

The silhouette of some Brazilian alkaline massifs is apparently similar to that of active volcanoes, generating local urban legends of volcano, such as the Mendanha, Morro de São João, and Cabugi Peak. The MCI parameter is strongly influenced by foothill angle of the massif and distinguishes well the both. The alkaline massifs has steep foothill slope with declivity of 30 to 35º, and their general three-dimensional landform is characteristically convex (Figure 11A). On the other hand, volcanoes has gentle foothill slope, with declivity lower than 10º, and their general form is concave (Figure 11B).

The summit level surface of alkaline massifs of the State of Rio de Janeiro is characterised by marginal scarp (MS, Figure 12), virtual plateau (VP), and top protrusion (TP). The virtual plateau is observed only on summit level maps and it is constituted, in fact, by high ridges and deep valleys. This map evidences the inexistence of volcanic cone and crater in Mendanha massif, that is, absence of 'Nova Iguaçu Volcano'.

Volume-normalised three-dimensional concavity index

The authors propose another morphologic parameter in order to represent general convexity of massifs, called volume-normalised three-dimensional concavity index (TCI).

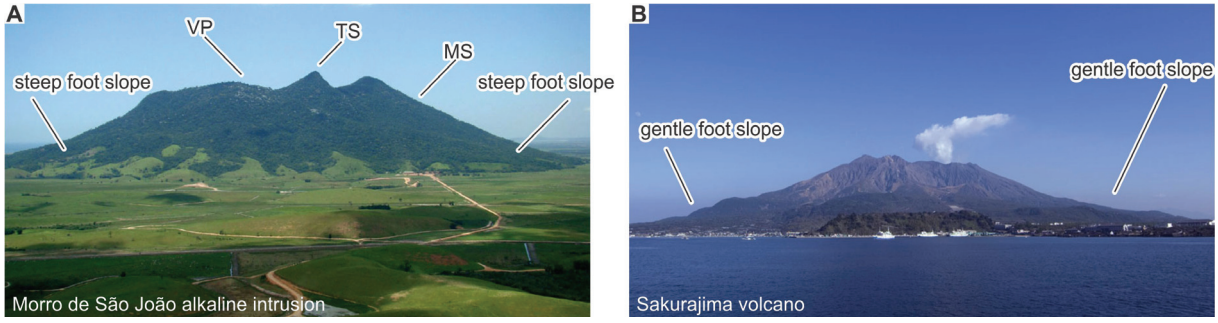

Figure 11. Apparent similarity of the mountain silhouette: A) Morro de São João alkaline intrusive massif, State of Rio de Janeiro, Brazil (GERALDES et al., 2013); B) Sakurajima active volcano, Province of Kagoshima, Japan. The photo B is credit of Junyoh Tanaka free of free license.

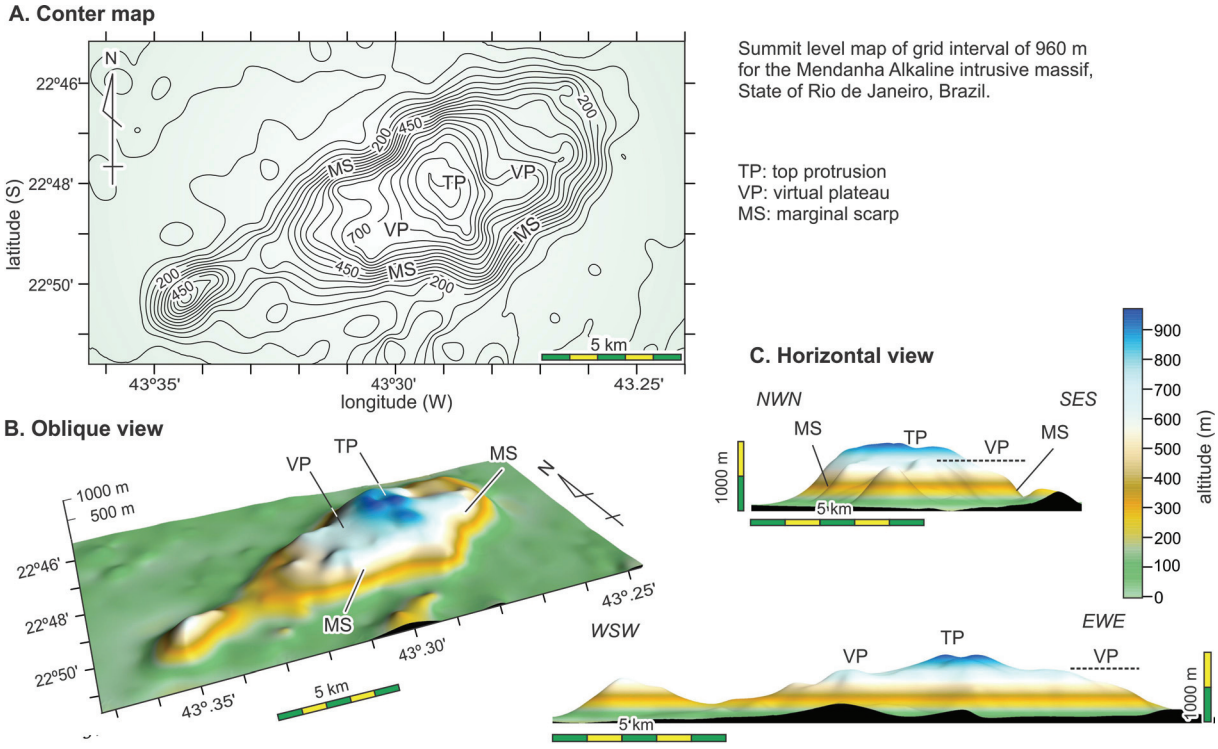

Figure 12. Summit lever surface based of grid interval of 960 m (A), its oblique view (B), and horizontal views (C), demonstrating the top protrusion (TP), virtual plateau (VP), and marginal scarp (MS). The original topographic data is originated from the Aster Gdem.

This parameter corresponds to three-dimensional expansion of area-normalised stream concavity index (DEMOULIN, 1998; ZAPROWSKI et al., 2005). The TCI is calculated by the equation: TCI = 1 -2 x V, where V is the volume of massif divided by that of envelope space (Figure 14A).

The data of close to the massif foot have strong influence of talus and fan deposits, and therefore, they are excluded. The data above this level represent erosive morphology and are called effective data. In practice, TCI is calculated using hypsometric diagram. In this case, the massif volume V corresponds to the sum of the normalised frequency of the effective data (Figure 14B). When TCI > 0, the massif has concave general three-dimensional form, and when TCI < 0, convex form.

The diagrams of TCI (Figure 13) vs. MCI (Figure 10) and TCI vs. R2 distinguish well the erosive characteristics of massifs according to constituent base rocks (Figure 14). The parameter R2 is coefficient of determination of the hypsometric diagram (Figure 13B). Among the massifs of Fluminense Lowland, State of Rio de Janeiro (Figure 4, 5), Pedra Branca granitic massif has high TCI, high MCI, and low R2, respectively 0.55, -0.4, and 0.78. Tijuca gneissic massif also has high TCI, high MCI, and low R2, respectively 0.54, -0.5, and 0.80. On the other hand, Morro de São João nepheline syenite massif has low TCI, low MCI, and high R2, respectively 0.20, -1.2, and 0.97 (Figure 14).

These diagrams show that the data of granitic and gneissic massifs and those of syenitic massifs are distributed in two distinctly separated areas. The data of Mendanha alkaline massif is projected in the intermediate area between the syenitic and granitic trends. The fact is attributed to the fact that the analysed area has either syenitic or gneissic rocks.

The Figure 13 shows the base level map of grid interval of 28 km for Vitória-Trindade Chain, exhibiting 3 basement elevations at Davis (DVS), Jaseur (JSR), and Congress (CGS) seamounts. The dome-like basement elevations are from 100 to 150 km of diameter and from 1000 to 1400 m of relative height. These diameters are significantly larger than those of the seamount foot. Skolotnev et al. (2010) attributed these morphologic elevations to pre-eruptive tectonic uplift of the basement, corroborating the model of solid-state penetration of asthenospheric hot-mantle along the old abyssal fracture zone from the west to the east. This idea is supported by the low Bouguer anomaly along Vitória-Trindade Chain, indicating thin lithospheric mantle(Figures 14 and 15).

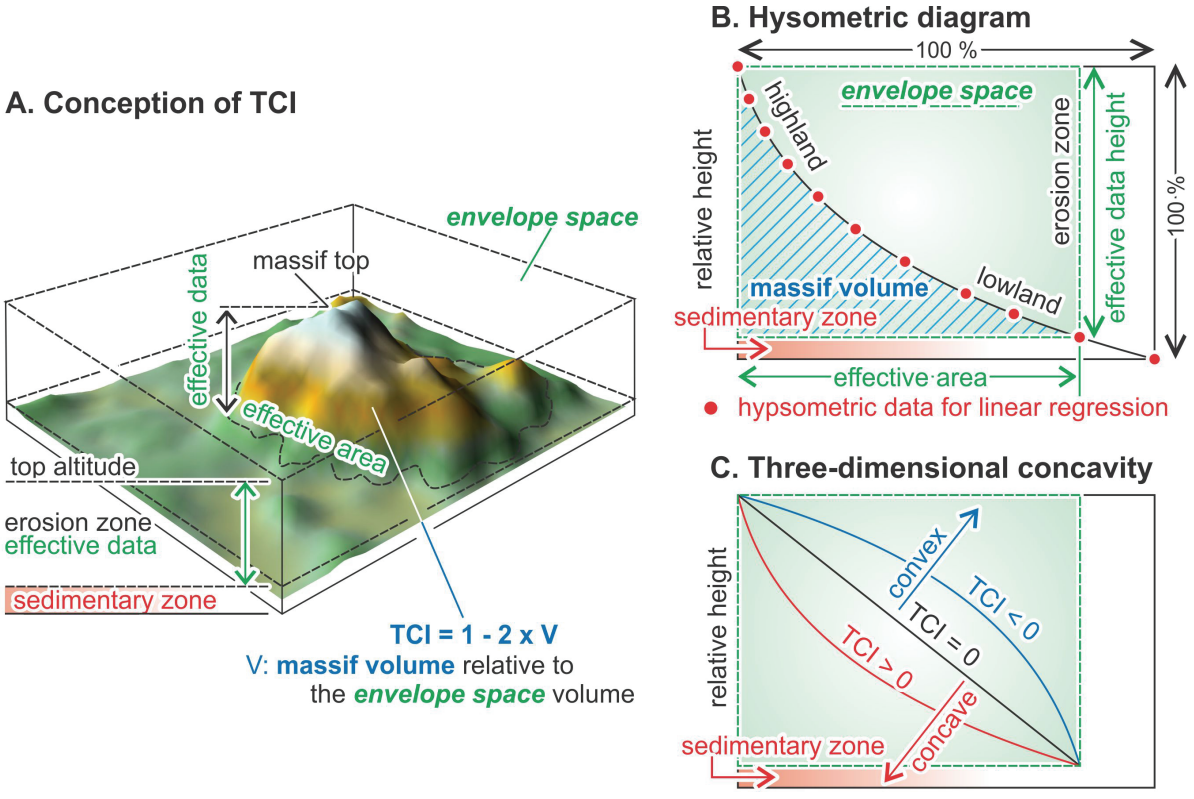

Figure 13. Principle of volume-normalised three-dimensional massif concavity index (TCI): A) Three-dimensional view explaining the conception of TCI: B) Hypsometric diagram and the parameter V, which represents relative volume; C) Relation between TCI and general concavity of the massif.

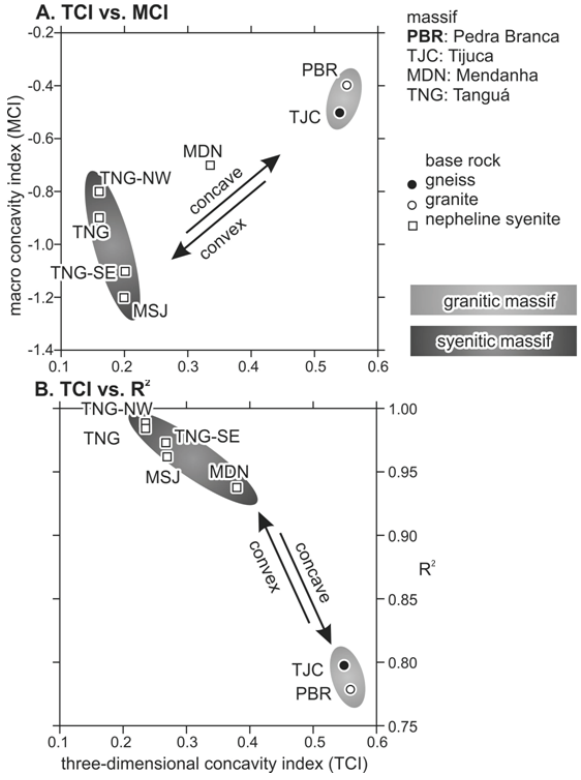

Figure 14. Erosive resistance discrimination diagram for Pedra Branca granitic massif, Tijuca gneissic massif, and felsic alkaline massifs of Tanguá e Morro de São João, State of Rio de Janeiro, Brazil: A) Volume-normalised three-dimensional concavity index (TCI) vs. macro concavity index (MCI); B) Volume-normalised three-dimensional concavity index (TCI) vs. coefficient of determination of hypsometric diagram (R^2).

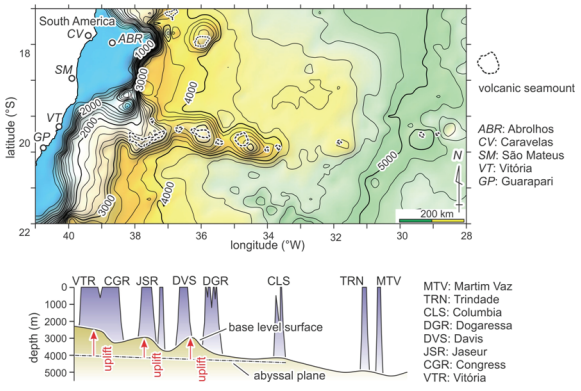

Figure 15. Base level map of grid interval of 27.8 km along Vitória-Trindade Chain, South Atlantic Ocean.

Conclusion

The available data and unpublished new data of the authors indicate the following utilities of summit level and base level techniques for geomorphologic studies.

1. Summit level (*seppômen*) is the virtual topographic surface constituted by local highest points, as peaks and ridges. This technique reconstitutes the palaeo-geomorphology before drainage erosion. It is efficient for reconstitution of palaeo-surface, detection of active tectonic movement, and geologic anomalies reflected to the landform.

2. Base level (*sekkokumen*) is the virtual surface composed of local lowest points, as valley bottoms. It predicts future morphology according to development of lateral erosion of the drainages. These virtual maps are constructed from the satellite digital topographic data of the Aster Gdem and SRTM, using the original software Baz and Wilbur.

3. The height difference between summit level and base level are called relief amount (*kifukuryô*) and indicates the degree of erosion of massifs in form of the MCI parameter. The massifs with high erosive resistance tend to have negative MCI and those of low resistance, positive MCI. This parameter distinguishes the landforms originated from volcano and differential erosion of intrusive massifs.

4. The volume-normalised three-dimensional concavity index, the TCI parameter, also represents general convexity of massifs. The massifs with high erosive resistance tend to have low TCI and MCI, and those with low resistance, high TCI and MCI. The diagram of TCI vs. MCI distinguishes erosive characteristics of massifs according to the constituent rocks.

5. The base level technique applied to ocean bottom morphology detects basement uplift before the formation of volcanic seamounts.

Acknowledgements

The present article is developed by the extension from Master Thesis of one of the authors Samuel da Silva, of the Department of Geology, Federal Fluminense University, Niterói, State of Rio de Janeiro, Brazil. The authors are grateful to the Faperj (Fundação de Amparo à Pesquisa do Estado do Rio de Janeiro, Carlos Chagas Filho), CNPq (Conselho Nacional de Desenvolvimento Científico e Tecnológico), Capes (Coordenação de Aperfeiçoamento de Pessoal de Nível Superior), and Petrobras (Petróleo do Brasil, S.A.) for the financial supports and scholarship.

Reference

AIRES, J. R.; MOTOKI, A.; MOTOKI, K. F.; MOTOKI, D. F.; RODRIGUES, J. G. Geomorphological analyses of the Teresópolis plateau and serra do mar cliff, State of Rio de Janeiro, Brazil with the help of summit level technique and aster gdem, and its relation to the cenozoic tectonism. **Anuário do Instituto de Geociências da**

Universidade Federal do Rio de Janeiro, v. 35, n. 2, p. 105-123, 2012.

ALMEIDA, F. F. M.; CARNEIRO, C. R. Origem e evolução da serra do mar. **Revista Brasileira de Geociências**, v. 28, n. 2, p. 135-150, 1998.

BENNIO, L.; BROTZU, P.; D'ANTONIO, M.; FERAUD, G.; GOMES, C. B.; MARZOLI, A.; MELLUSO, L.; MORBIDELLI, L.; MORRA, V.; RAPAILLE, C.; RUBERTI, E. The tholeiitic dyke swarm of the arraial do cabo peninsula (SE Brazil): $^{39}Ar/^{40}Ar$ ages, petrogenesis, and regional significance. **Journal of South American Earth Sciences**, v. 16, n. 2, p. 163-176, 2003.

BROTZU, P.; BECCALUVA, L.; CONTE, A.; FONSECA, M.; GARBARINO, C.; GOMES, C. B.; LEONG, R.; MACCIOTTA, G.; MANSUR, R. L.; MELLUSO, L.; MORBIDELLI, L.; RUBERTI, E.; SIGOLO, J. B.; TRAVERSA, G.; VALENÇA, J. G. Petrological and geochemical studies of alkaline rocks from continental Brazil. The syenitic intrusion of Morro Redondo, RJ. **Geochimica Brasiliensis**, v. 3, n. 1, p. 63-80, 1989.

BROTZU, P.; GOMES, C. B.; MELLUSO, L.; MORBIDELLI, L.; MORRA, V.; RUBERTI, E. Petrogenesis of coexisting SiO_2-undersaturated to SiO_2-oversaturated felsic igneous rocks: the alkaline complex of Itatiaia, southern eastern Brazil. **Lithos**, v. 40, n. 2-4, p. 133-156, 1997.

BROTZU, P.; MELLUSO, L.; BENNIO, L.; GOMES, C. B.; LUSTRINO, M.; MORBIDELLI, L.; MORRA, V.; RUBERTI, E.; TASSINARI, C.; D'ANTONIO, M. Petrogenesis of the early cenozoic potassic alkaline complex of morro de São João, southeastern Brazil. **Journal of South American Earth Sciences**, v. 24, n. 1, p. 93-115, 2007.

CAMPOS, T. F. C.; BEZERRA, F. H. R.; SRIVASTAVA, N. K.; VIEIRA, M. M.; VITA-FINZI, C. Holocene tectonic uplift of the St. Peter and St. Paul Rocks (Equatorial Atlantic), consistent with emplacement by extrusion. **Marine Geology**, v. 271, n. 1-2, p. 177-186, 2010.

COUTO, E. V.; FROTES, E.; SORDI, M. V.; MARQUES, A. J.; CAMOLEZI, B. A. Seppômen maps for geomorphic developments analysis: the case of Paraná plateau border, Faxinal, State of Paraná, Brazil. **Acta Scientiarum. Technology**, v. 34, n. 1, p. 71-78, 2012.

DAVIS, W. M. The geographical cycle. **Geographical Journal of the Royal Geographical Society**, v. 14, n. 5, p. 481-504, 1899.

DEFFONTAINES, B.; LEE, J. C.; ANGELIER, J., VARVALHO, J.; RUDANT, J. P. New geomorphic data on the active Taiwan orogen: A multisource approach. **Journal of Geophysical Research**, v. 99, n. B10, p. 20243-2066, 1994.

DEMOULIN, A. Testing the tectonic significance of some parameters of longitudinal river profiles: the case of the Ardenne (Belgium, NW Europe), **Geomorphology**, v. 24, n. 5, p. 189-208, 1998.

DERBY, O. A. On nepheline-rocks in Brazil - part II. The Tinguá mass. **The Quarterly Journal of the Geological Society of London**, v. 47, n. 1, p. 251-265, 1897.

FERHAT, G.; FEIGL, K. L.; RITZ, J. F.; SOURIAU, A. Geodetic measurement of tectonic deformation in the southern alps and provence, France, 1947-1994. **Earth and Planetary Science Letters**, v. 159, n. 1-2, p. 35-46, 1998.

FERRARI, A. L. **Evolução tectônica do graben da Guanabara**. São Paulo: Instituto de Geociências/USP, 2001.

GERALDES, M. C.; MOTOKI, A.; VARGAS, T.; IWANUCH, W.; BALMANT, A.; MOTOKI, K. F. Geology, petrography, and emplacement mode of the Morro dos Gatos alkaline intrusive rock body, State of Rio de Janeiro, Brazil. **Geociências**, v. 32, n. 4, p. 625-639, 2013.

HEILBRON, M., MACHADO, N. Timing of terrane accretion in the neoproterozoic-eopaleozoic ribeira orogen (se Brazil). **Precambrian Research**, v. 125, n. 1-2, p. 87-112, 2003.

HEILBRON, M.; MOHRIAK, W.; VALERIANO, C. M.; MILANI, E. J.; ALMEIDA, J. C. A.; TUPINAMBÁ, M. From collision to extension: the roots of the southeastern continental margin of Brazil. In: MOHRIAK, W. U.; TALWANI, M. (Ed.). **Geophysical monograph**. Washington, D.C.: American Geophysical Union, 2000. p. 1-32.

HUZITA, K.; KASAMA, T. **Kôbe oyobi rinsetsu chiiki chisitu-zu, 1/50,000 (Geologic map of kobe and the adjacent area, 1/50.000)**. Geologic map. 3rd ed. Japan: Secretary of Planning, Municipal District of Kobe, 1977.

KÜHNI, A.; PFIFFNER, O. A. The relief of the swiss alps and adjacent areas and its relation to lithology and structure: topographic analysis from a 250-m DEM. **Geomorphology**, v. 41, n. 4, p. 285-307, 2001.

LIN, A. M.; MARUYAMA, T.; MIYATA, T. Fushimi large earthquake produced by a slip on the Gosukebashi fault at the eastern rokko mountains, Japan. **Island Arc**, v. 7, n. 4, p. 621-636, 1998.

MACDONALD, W. D.; PALMER, H. C. Flow directions in ash-flow tuffs: a comparison of geological and magnetic suspectibiligy measurements, tshirego memger (upper Bandelier Tuff), Valles Caldera, New Mexico, USA. **Bulletin of Volcanology**, v. 53, n. 1, p. 45-59, 1990.

MALENGREAU, B.; LÉNAT, J. F.; FROGER, J. L. Structure of réunion island (Indian Ocean) inferred from the interpretation of gravity anomalies. **Journal of Volcanology and Geothermal Research**, v. 88, n. 3, p. 131-146, 1999.

MARTIN, R. Paleogeomorphology and its application to exploration for oil and gas (with examples from western Canada). **American Association of Petroleum Geology Bulletim**, v. 50, n. 10, p. 2277-2311, 1966.

MARUYAMA, T.; LIN, A. M. Tectonic history of the rokko active fault zone (southwest Japan) as inferred from cumulative offsets of stream channels and basement rocks. **Tectonophysics**, v. 323, n. 3-4, p. 197-216, 2000.

MOTOKI, A. A possible fossil earthquake swarm? - Relationship between mesozoic basaltic dykes and their linkage faults. **Journal of Geography**, v. 103, n. 3, p. 548-557, 1994.

MOTOKI, A. Cretaceous volcanic vents in southeast part of Mt. Rokko, western Honshu, Japan. **Bulletin of the Volcanological Society of Japan**, v. 24, n. 2, p. 55-72, 1979.

MOTOKI, A.; NEVES, J. L. P.; VARGAS, T. Quantitative colour analyses using digital specification technique for mármore bege Bahia, a representative Brazilian ornamental limestone of breccia-like texture. **Revista Escola de Minas**, v. 58, n. 2, p. 113-120, 2005.

MOTOKI, A.; SICHEL, S. E. Avaliação de aspectos texturais e estruturais de corpos vulcânicos e subvulcânicos e sua relação com o ambiente de cristalização, com base em exemplos do Brasil, Argentina e Chile. **REM-Revista Escola de Minas**, v. 59, n. 1, p. 13-23, 2006.

MOTOKI, A.; ZUCCO, L. L.; SICHEL, S. E.; NEVES, J. L.; AIRES, J. R. Development of the technique for digital colour specification and the new nomenclatures of ornamental rock based on the measured colours. **Geociências**, v. 26, n. 2, 151-160, 2006.

MOTOKI, A.; PETRAKIS, G. H.; SOARES, R. S.; SICHEL, S. E.; AIRES, J. R. New method of semi-automatic modal analyses for phenocrysts of porphyritic rocks based on quantitative digital colour specification technique. **REM-Revista Escola de Minas**, v. 60, n. 1, p. 13-20, 2007a.

MOTOKI, A.; SOARES, R.; NETTO, A. M.; SICHEL, S. E.; AIRES, J. R.; LOBATO, M. Genetic reconsideration of the Nova Iguaçu volcano model, State of Rio de Janeiro, Brazil: Eruptive origin or subvolcanic intrusion? **REM-Revista Escola de Minas**, v. 60, n. 4, p. 583-592, 2007b.

MOTOKI, A.; SOARES, R.; NETTO, A. M.; SICHEL, S. E.; AIRES, J. R.; LOBATO, M. Geologic occurrence shape of pyroclastic rock dykes in the Dona Eugênia River Valley, Municipal Park of Nova Iguaçu, Rio de Janeiro. **Geociências**, v. 26, n. 1, p. 67-82, 2007c.

MOTOKI, A.; SOARES, R. S.; LOBATO, M.; SICHEL, E. S.; AIRES, J. R. Weathering fabrics in felsic alkaline rocks of Nova Iguaçu, State of Rio de Janeiro, Brazil. **REM-Revista Escola de Minas**, v. 60, n. 3, p. 451-458, 2007d.

MOTOKI, A.; SICHEL, S. E. Hydraulic fracturing as possible mechanism of dyke-sill transition and horizontal discordant intrusion: An example of Arraial do Cabo area, State of Rio de Janeiro, Brazil. **Geofísica Internacional**, v. 47, n. 1, p. 13-25, 2008.

MOTOKI, A.; PETRAKIS, G. H.; SICHEL, S. E.; CARDOSO, C. E.; MELO, R. C.; SOARES, R. S.; MOTOKI, K. F. Landform origin of the mendanha syenitic massif, State of Rio de Janeiro, Brazil, based on the geomorphological analyses by summit level map technique. **Geociências**, v. 27, n. 1, p. 99-115, 2008a.

MOTOKI, A.; SICHEL, S. E.; SOARES, R. S.; NEVES, J. L. P.; AIRES, J. R. Geological, lithological, and petrographical characteristics of the Itaúna alkaline intrusive complex, São Gonçalo, State of Rio de Janeiro, Brazil, with special attention of its emplace mode. **Geociências**, v. 27, n. 1, p. 33-44, 2008b.

MOTOKI, A.; SICHEL, S. E.; SAVI, D. C.; AIRES, J. R. Intrusion mechanism of tabular intrusive bodies of subhorizontal discordant emplacement of the Cabo Frio Island and the neighbour areas, State of Rio de Janeiro, Brazil. **Geociências**, v. 27, n. 2, p. 207-218, 2008c.

MOTOKI, A.; SICHEL, S. E.; SOARES, R. S.; AIRES, J. R.; SAVI, D. C.; PETRAKIS, G. H.; MOTOKI, K. F. Vent-filling pyroclastic rocks of the mendanha, the Itaúna, and the Cabo Frio Island, State of Rio de Janeiro, Brazil, and their formation process based of the conduit implosion model. **Geociências**, v. 27, n. 3, 451-467, 2008d.

MOTOKI, A.; SICHEL, S. E.; CAMPOS, T. F. C.; SRIVASTAVA, N. K.; SOARES, R. S. Present-day uplift rate of the Saint Peter and Saint Paul Islets, Equatorial Atlantic Ocean. **Revista Escola de Minas**, v. 62, n. 3, p. 331-342, 2009a.

MOTOKI, A.; SICHEL, S. E.; PETRAKIS, G. H. Genesis of the tabular xenoliths along contact plane of the mafic dykes of Cabo Frio area, state of Rio de Janeiro, Brazil: Thermal delamination or hydraulic shear fracturing? **Geociências**, v. 27, n. 2, p. 207-218, 2009b.

MOTOKI, A.; SICHEL, S. E.; VARGAS, T.; AIRES, J. R.; IWANUCH, W.; MELLO, S. L. M.; MOTOKI, K. F.; SILVA, S.; BALMANT, A.; GONÇALVES, J. Geochemical evolution of the felsic alkaline rocks of Tanguá, Rio Bonito, and Itaúna intrusive bodies, State of Rio de Janeiro, Brazil. **Geociências**, v. 29, n. 3, p. 291-310, 2010.

MOTOKI, A.; VARGAS, T.; IWANUCH, W.; SICHEL, S. E.; BALMANT, A.; AIRES, J. R. Tectonic breccia of the Cabo Frio area, State of Rio de Janeiro, Brazil, intruded by early cretaceous mafic dyke: Evidence of the Pan-African brittle tectonism? **REM-Revista Escola de Minas**, v. 64, n. 1, p. 25-36, 2011.

MOTOKI, A.; CAMPOS, T. F. C.; FONSECA, V. P.; MOTOKI, K. F. Subvolcanic neck of Cabugi Peak, State of Rio Grande do Norte, Brazil, and origin of its landform. **Revista Escola de Minas**, v. 65, n. 1, p. 35-45, 2012a.

MOTOKI, A., MOTOKI, K. F., MELO, D. P. Submarine morphology characterization of the Vitória-Trindade Chain and the adjacent areas, State of Espírito Santo, Brazil, based on the predicted bathymetry of the TOPO version 14.1. **Revista Brasileira de Geomorfologia**, v. 13, n. 2, p. 151-170, 2012b.

MOTOKI, A.; GERALDES, M. C.; IWANUCH, W.; VARGAS, T.; MOTOKI, K. F.; BALMANT, A.; RAMOS, M. N. The pyroclastic dyke and welded crystal tuff of the Morro dos Gatos alkaline intrusive complex, State of Rio de Janeiro, Brazil. **REM-Revista Escola de Minas**, v. 65, n. 1, p. 35-45, 2012c.

MOTOKI, A.; VARGAS, T.; IWANUCH, W.; MELO, D. P.; SICHEL, S. E.; BALMANT, A.; AIRES, J. R.; MOTOKI, K. F. Fossil earthquake evidenced by the silicified tectonic breccia of the Cabo Frio area, State of Rio de Janeiro, Brazil, and its bearings on the genesis of

stick-slip fault movement and the associated amagmatic hydrothermalism. **Anuário do Instituto de Geociências da Universidade Federal do Rio de Janeiro**, v. 35, n. 2, p. 124-139, 2012d.

MOTOKI, A.; SILVA, S.; SICHEL, S. E.; MOTOKI, K. F. Geomorphological analyses by summit level and base level maps based on the aster gdem for Morro de São João felsic alkaline Massif, State of Rio de Janeiro, Brazil. **Geociências**, v. 33, n. 1, p. 11-25, 2014a.

MOTOKI, K. F.; MOTOKI, A.; SICHEL, S. E. Gravimetric structure for the abyssal mantle exhumation massif of Saint Peter and Saint Paul peridotite ridge, Equatorial Atlantic ocean, and its relation to the active uplift driving force. **Anais de Academia Brasileira de Ciências**, v. 86, n. 2, p. 571-588, 2014b.

MOTOKI, A.; SICHEL, S. E.; SILVA, S.; MOTOKI, K. F. Morphologic characteristics and erosive resistance of felsic alkaline intrusive massif of Tanguá, State of Rio de Janeiro, Brazil, based on the aster gdem. **Geociências**, v. 34, n. 1, p. 19-31, 2015a.

MOTOKI, A.; SICHEL, S. E.; SILVA, S.; MOTOKI, K. F.; RIBEIRO, A. K. Drainage erosion and concave landform of Tijuca gneissic massif, State of Rio de Janeiro, Brazil, with the help of summit level and base level technique based on Aster Gdem. **Geociências**, v. 34, n. 1, p. 116-129, 2015b.

OKUMA, S.; STOTTER, C.; SUPPER, R.; NAKATSUKA, T.; FURUKAWA, R.; MOTSCHKA, K. Aeromagnetic constraints on the subsurface structure of Stromboli volcano, Aeolian Islands, Italy. **Tectonophysics**, v. 478, n. 1-2, p. 19-33, 2009.

PETRAKIS, G. H.; MOTOKI, A.; SICHEL, S. E.; ZUCCO, L. L.; AIRES, J. R.; MELLO, S. L. M. Ore geology of special quality gravel and artificial sand: Examples of alkaline syenite of Nova Iguaçu, State of Rio de Janeiro, and rhyolite of Nova Prata, State of Rio Grande do Sul, Brazil. **Geociências**, v. 29, n. 1, p. 21-32, 2010.

PIRES, G. L. C.; BONGIOLO, E. M.; NEUMANN, R.; ÁVILA, C. A. Caracterização petrográfica e mineralógica de brechas magmático-hidrotermais no complexo alcalino de Itatiaia, Estado do Rio de Janeiro: Ocorrências de fluorita e minerais de ETR. **Anuário do Instituto de Geociências da Universidade Federal do Rio de Janeiro**, v. 37, n. 1, p. 5-16, 2014.

RICCOMINI, C.; SANT'ANNA, L. G.; FERRARI, A. L. Evolução geológica do rift continental do Sudeste do Brasil. In: MANTESSO-NETO, V.; BARTORELLI, A.; CARNEIRO, C. D. R.; BRITO-NEVES, B. B. (Ed.). **Geologia do continente Sul-Americano**: Evolução da obra de Fernando Flávio Marques de Almeida. São Paulo: Beca, 2004. p. 385-405.

RIIS, F. Quantification of cenozoic vertical movements of scandinavia by correlation of morphological surfaces with offshore data. **Global and Planetary Change**, v. 12, n. 1-4, p. 331-357, 1996.

RÖMER, W. Accordant summit heights, summit levels and the origin of the "upper denudation level" in the Serra do Mar (SE-Brazil, São Paulo): A study of hillslope forms and processes. **Geomorphology**, v. 100, n. 3-4, p. 312-327, 2008.

RUST, D.; BEHNCKE, B.; NERI, M.; CIOCANEL, A. Nested zones of instability in the Mount Etna volcanic edifice, Italy. **Journal of Volcanology and Geothermal Research**, v. 144, n. 1-4, p. 137-153, 2005.

SATO, H.; RAIM, R. Landform analysis using summit level and streamline surface in Abukuma mountains. **Transactions of Japanese Geomorphological Union**, v. 23, n. 3, p. 480-481, 2004.

SICHEL, S. E.; ESPERANÇA, S.; MOTOKI, A.; MAIA, M.; HORAN, M. F.; SZATMARI, P.; ALVES, E. C.; MELLO, S. L. M. Geophysical and geochemical evidence for cold upper mantle beneath the Equatorial Atlantic Ocean. **Brazilian Journal of Geophysics**, v. 26, n. 1, p. 69-86, 2008a.

SICHEL, S. E.; MOTOKI, A.; SAVI, D. C.; SOARES, R. S. Subvolcanic vent-filling welded tuff breccia of the Cabo Frio Island, State of Rio de Janeiro, Brazil. **REM-Revista Escola de Minas**, v. 61, n. 4, p. 423-432, 2008b.

SICHEL, S. E.; MOTOKI, A.; ANGEL-AMAYA, J.; VARGAS, T.; MAIA, M.; CAMPOS, T. F. C.; BAPTISTA NETO, J. A.; KOGA, M. S.; MOTOKI, K. F.; SIMÕES, L. S. A.; SZATMARI, P. Origem e evolução das rochas mantélicas da cadeia peridotítica de São Pedro e São Paulo, oceano Atlântico Equatorial. **Boletim de Geociências da Petrobras**, v. 20, n. 1-2, p. 97-128, 2011.

SICHEL, S. E.; MOTOKI, A.; IWANUCH, W.; VARGAS, T.; AIRES, J. R.; MELO, D. P.; MOTOKI, K. F.; BALMANT, A.; RODRIGUES, J. G. Fractionation crystallisation and continental crust assimilation by the felsic alkaline rock magmas of the State of Rio de Janeiro, Brazil. **Anuário do Instituto de Geociências da Universidade Federal do Rio de Janeiro**, v. 35, n. 2, p. 84-104, 2012.

SILVA, S. **Interpretação morfológica baseada nas tecnicas de seppômen e sekkokumen dos maciços alcalinos do Estado do Rio de Janeiro**. Niterói: Instituto de Geociências/UFF, 2010.

SKOLOTNEV, S. G.; PEYVE, A.; TRUKO, N. N. New data on the structure of the Vitoria-Trindade seamount chain (western Brazil basin, South Atlantic). **Doklady Earth Sciences**, v. 431, n. 2, p. 435-440, 2010.

SMITH, R. L.; BAILEY, R. A. The bandelier tuff: A study of ash-flow eruption cycles from zoned magma chambers. **Bulletin of Volcanology**, v. 29, n. 1, p. 83-104, 1966.

SMITH, W. H.; SANDWELL, D. T. Bathymetric prediction from dense satellite altimetry and sparse shipboard bathymetry. **Journal of Geophysical Research**, v. 99, n. B2, p. 21803-21824, 1994.

SUZUKI-KAMATA, K.; KAMATA, H. The proximal facies of the Tosu pyroclastic-flow deposit erupted from Aso caldera, Japan. **Bulletin of Volcanology**, v. 52, n. 5, p. 325-333, 1990.

ULBRICH, H. H. G. J. **A petrografia, a estrutura e quimismo de nefelina sienitos do maciço alcalino de Poços de Caldas, MG-SP**. São Paulo: Instituto de Geociências/USP, 1984.

VALERIANO, C. M.; TUPINAMBÁ, M.; SIMONETTI, A.; HEILBRON, M.; ALMEIDA, J. C. H.; EIRADO, L. G. U-Pb LA-MC-ICPMS geochronology of Cambro-Ordovician post-collisional granites of the ribeira belt, southeat Brazil: Terminal brasiliano magmatism in central gondwana supercontinent. **Journal of South American Earth Sciences**, v. 32, n. 4, p. 416-428, 2011.

VALLADARES, C. S.; MACHADO, N.; HEILBRON, M.; DUARTE, B. P.; GAUTHIER, G. Sedimentary provenance in the central ribeira belt based on laser-ablation. **Gondwana Research**, v. 13, n. 4, p. 516-526, 2008.

VILARDO, G.; NATALE, G.; MILANO, G.; COPPA, U. The seismicity of Mt. Vesuvius. **Tectonophysics**, v. 261, n. 1-3, p. 127-138, 1996.

WATANABE, K. Studies on the aso pyroclastic flow deposits in the region to the west of aso caldera, southwest Japan, I: Geology. **Memoirs of the Faculty of Education, Kumamoto University, Natural science**, v. 27, n. 1-3, p. 97-120, 1978.

YOKOYAMA, I. Preliminary report on a gravimetric survey on toya caldera, Hokkaido, Japan. **Journal of the Fuculty of Science, Hokkaido University**, v. 2, n. 2, p. 247-250, 1965.

YOKOYAMA, I. Some remarks on calderas. **Bulletin of the Volcanological Society of Japan**, v. 14, n. 2, p. 77-83, 1969.

YOKOYAMA, I.; SAITO, T. Preliminary report on a gravimetric survey on volcano Hakone, Japan. **Journal of the Fuculty of Science, Hokkaido University**, v. 2, n. 2, p. 239-245, 1965.

YOKOYAMA, I.; TAJIMA, H. A gravity survey on volcano Huzi, Japan by means of a worden gravimeter. **Pure and Applied Geophisics**, v. 45, n. 1, p. 1-12, 1960.

YOKOYAMA, I.; TAJIMA, H. Gravity survey on the Kuttyaro caldera by means of a worden gravimeter. **Nature**, v. 183, n. 739, p. 739-740, 1959.

ZALÁN, P. V.; OLIVEIRA, J. A. B. Origem e evolução estrutural do sistema de riftes cenozóicos do sudeste do Brasil. **Boletim de Geociências da Petrobras**, v. 13, n. 2, p. 269-300, 2005.

ZAPROWSKI, B., PAZZAGLIA, F., EVENSON, E. Climatic influences on profile concavity and river incision. **Journal of Geophysical Research**, v. 110, F03004, 2005. doi:10.1029/2004JF000138.

Received on March 31, 2013.
Accepted on May 3, 2014.